Supporting Information

Ao Chen[a], Xun Guo[a], Shuo Yang[a], Guojing Liang[a], Qing Li[a], Ze Chen[a], Zhaodong Huang[a], Qi Yang[a,c], Cuiping Han[a*], Chunyi Zhi[a,b,c*]

[a] Department of Materials Science and Engineering, City University of Hong Kong, 83 Tat Chee Avenue, Kowloon, Hong Kong, China

[b] Centre for Functional Photonics, City University of Hong Kong, 83 Tat Chee Avenue, Kowloon, Hong Kong, 999077, China

[c] Hong Kong Center for Cerebro-Cardiovascular Health Engineering (COCHE), Pak Shek Kok, Shatin, NT, HKSAR, China

1. Experimental section

Battery fabrication: commercial $LiCoO_2$ and graphite were employed as the cathode and anode materials, respectively. The commercial copper foil (8 μm thickness) and aluminum foil (15 μm thickness) were used as the cathode current collector and anode current collector, respectively. Typically, the cathode was prepared by coating the slurry that mixed $LiCoO_2$ powers, super p (conductive agent) and polyvinylidene fluoride PVDF (90:5:5 wt/wt/wt) on the aluminum foil. The anode was prepared by coating the slurry that mixed graphite, super p and carboxymethylcellulose sodium (CMC) (93:2:5) on the copper foil. Then, the electrodes were dried in a vacuum oven at 70 ^{o}C for 12 h and compacted by a roller press. To prepare the flexible lithium ion batteries, the electrodes and separators (Celgard 2325) were cut into required size. Then, the multilayer structure comprising cathode/separator/anode was segmented into a plurality of interconnected segments, and each segment was folded in half. Then, the folded segment can be winded into cubic unit, and a flexible battery with cubic units can be obtained by winding all the folded segments. By using different winding methods, the interconnected energy storage units with cylindrical or triangle prism shape could be obtained. Finally, the battery was sealed by aluminum-plastic film and using the 1 M $LiPF_6$ in the ethylene carbonate/diethyl carbonate (1:1 vol/vol) as the electrolyte in an argon-filled glovebox (O_2 < 0.1 ppm, H_2O < 0.1 ppm). For stretchable battery with cylindrical units, the sealed battery is packaged with an elastic silicone film.

Finite element simulation: The various deformations of flexible batteries with cubic and cylindrical units were simulated using 3D nonlinear finite element method, implemented in commercial software ABAQUS. In all cases, a 4-node quadrilateral stress/displacement elements with reduced integration were used. The thick energy storage units were considered as rigid parts. The linear isotropic elasticity was used for the battery structure with effective modulus and Poisson ratio. For batteries with cubic and cylindrical units, the length between the two units is 2 mm and 3 mm, respectively. The thickness of copper foil, separator and aluminum foil are 8 μm, 25 μm and 15 μm, respectively. 1 atm pressure was loaded on sides of copper and aluminum foil to simulate the vacuum conditions inside the pouch cell.

Characterization and electrochemical measurements: The flexible $LiCoO_2$/Graphite batteries firstly underwent a formation process. Typically, the batteries were charged to 3.5 V at 0.03C and then charged to 4.2 V at 0.1C. Galvanostatic discharge-charge tests were conducted on Land or Neware Battery Measurement System in the range of 2.8 to 4.2 V. A FEI XL30 Sirion SEM was used to investigate the morphologies of samples. Dynamic mechanical loading was performed by the customized battery bending tester and battery torsion tester. The dynamic bending test was carried out by Battery Bending Tester (KEJINGDA KJD-WQ-0513). The dynamic twisting test was carried out

By Battery Torsion Tester (KEJINGDA KJD-NZ-0512). The battery with at least 8 cubic units is employed to test the cycling performance under dynamic mechanical loading, and the length of the battery is preferably greater than 10cm. The battery with at least 8 cylindrical units is used to be test the cycling performance under dynamic mechanical loading.

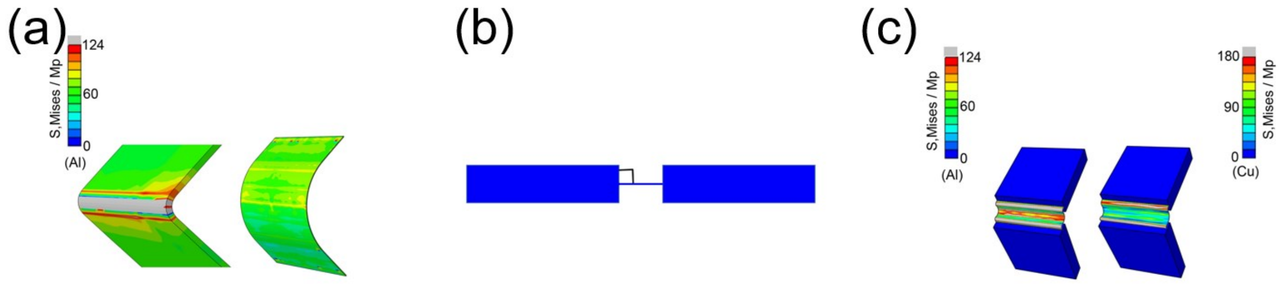

Figure S1. (a) Finite element simulation about the stress distribution of Al foil current collectors with 100 μm bending radius. (b) Conventional structure of flexible battery. (c) Finite element simulation results of the conventional structure with small torsional angle (45°). Gray means the stress exceeds the yield strength, leading to the plasmatic deformation

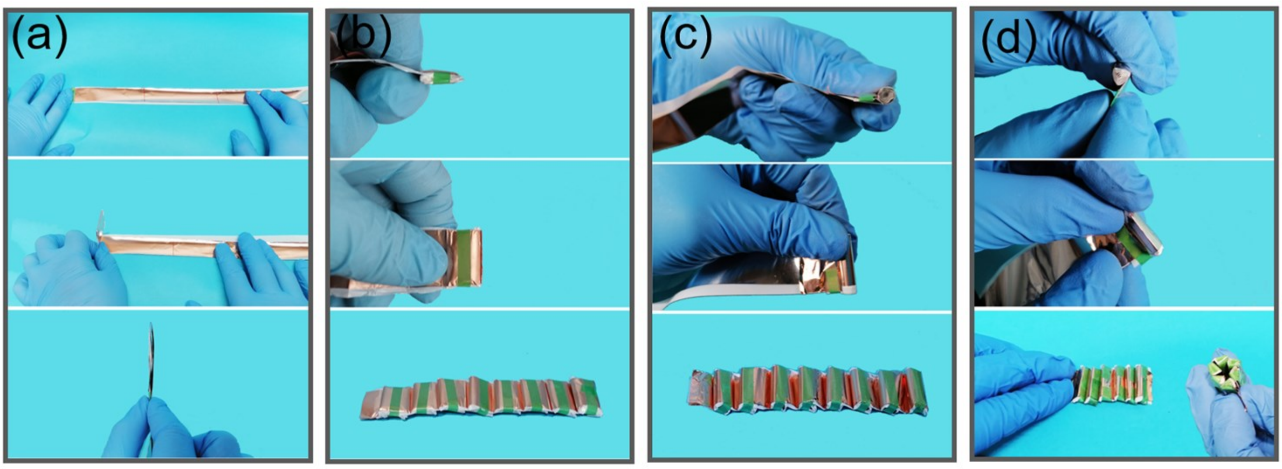

Figure S2. (a) The electrodes and separator were cut into required size. The multilayer structure comprising cathode/separator/anode was segmented into a plurality of interconnected segments, and the segment was folded in half. (b) Cubic unit can be obtained by winding the folded segment and battery with cubic units can be obtained by winding all the folded segments. (c) By winding the folded segment, the battery with cylindrical units can be obtained. (d) By winding the folded segment, the battery with triangular prism shaped units can be obtained.

Supplementary note 1

2. Calculations of theoretical relative energy density of the battery with cubic units

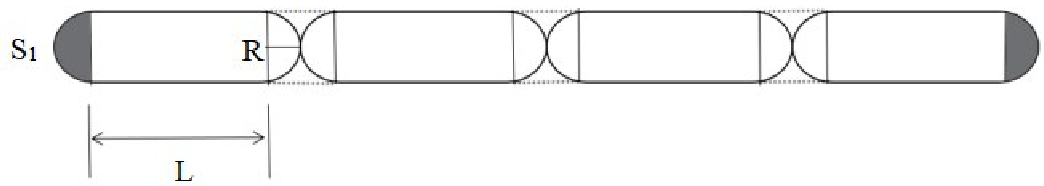

Figure S3. Structure of the battery.

To simplify the battery model, we only draw 4 cubic units. We set the number of cubic units as n and set the area of the end part of the battery as S1. We set Sb as the whole cross-sectional area of the battery and Sa as the cross-sectional area of conventional battery.

$$S1 = \frac{1}{2}\pi\left(\frac{R}{2}\right)^2 = \frac{\pi R^2}{8};$$

$$S_{\mathrm{b}} = 2nS_1 + nLR;$$

$$S_a = ((n-1)R + nL)\times R + 2S_1$$

L is the length of cubic unit; R is the thickness of cubic unit. We set the relative energy density as k.

$$k = \frac{S_{\mathrm{b}}}{S_a} = \frac{\frac{\pi}{4} + \frac{L}{R}}{1 + \frac{L}{R} + \frac{\pi - 4}{4\mathrm{n}}}$$

To simplify the calculation, when n > 4 we set $k \approx \frac{\frac{\pi}{4} + \frac{L}{R}}{1 + \frac{L}{R}}$

So, as shown in **Figure S4**, the relative energy density increases with the value of L/R.

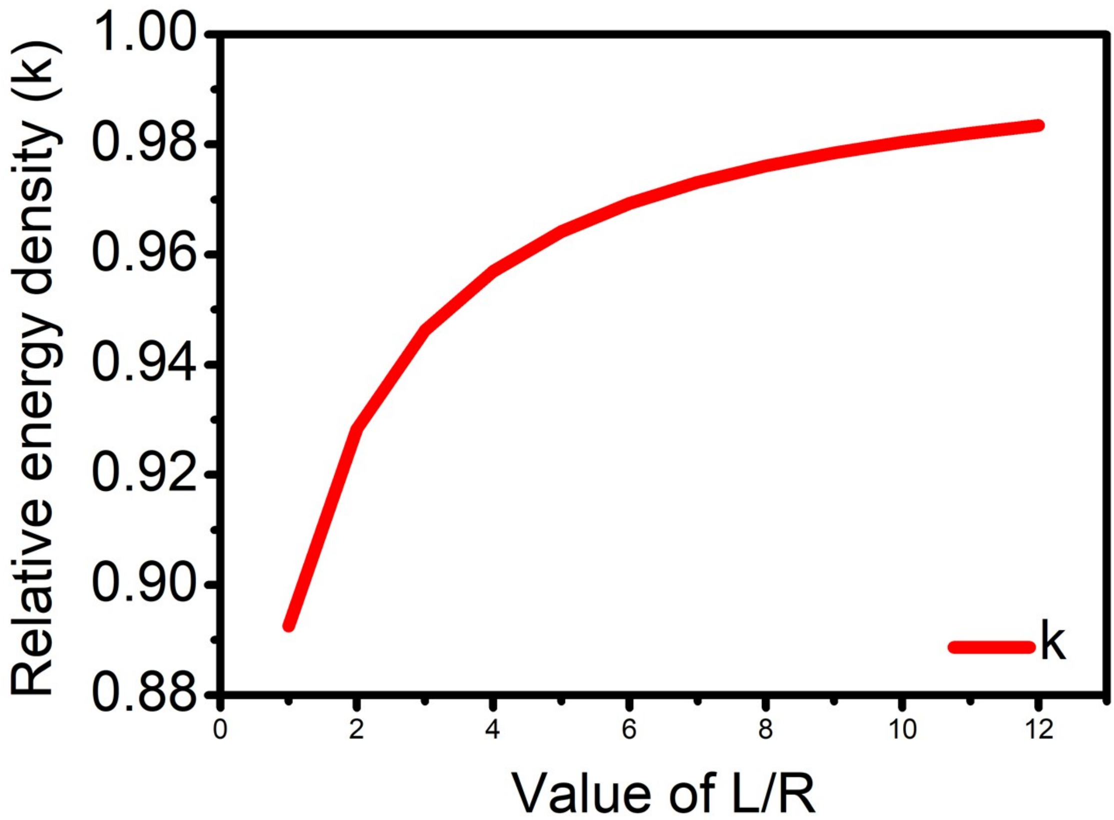

Figure S4. The relation between k and L/R. As the value of L/R increases, the relative energy density can easily exceed 90%.

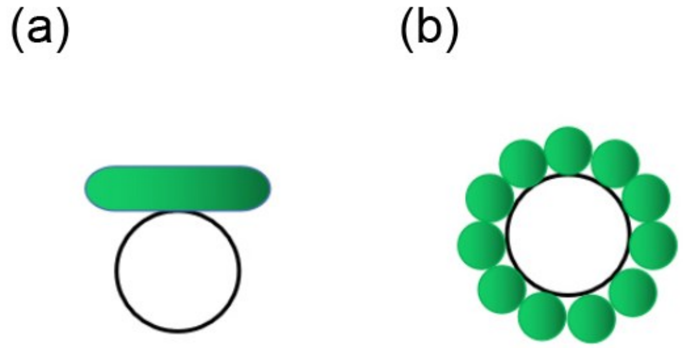

Figure S5. (a) Surface-to-point contact between cubic unit and cambered surface. (b) Point-to-point contact between cylindrical unit and cambered surface.

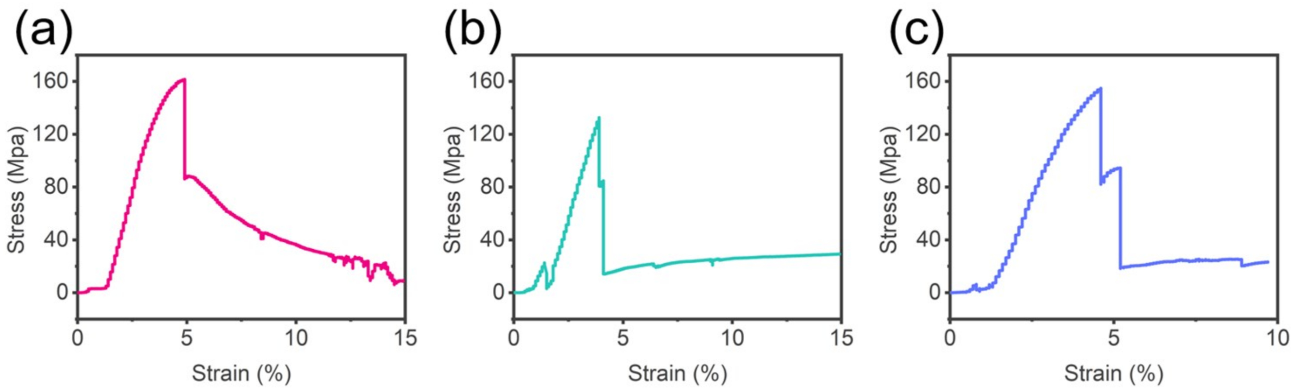

Figure S6. Tensile stress/strain curves for the (a) flexible battery with cubic units and (b) flexible battery with cylindrical units and (c) flexible battery with triangular prism shaped units.

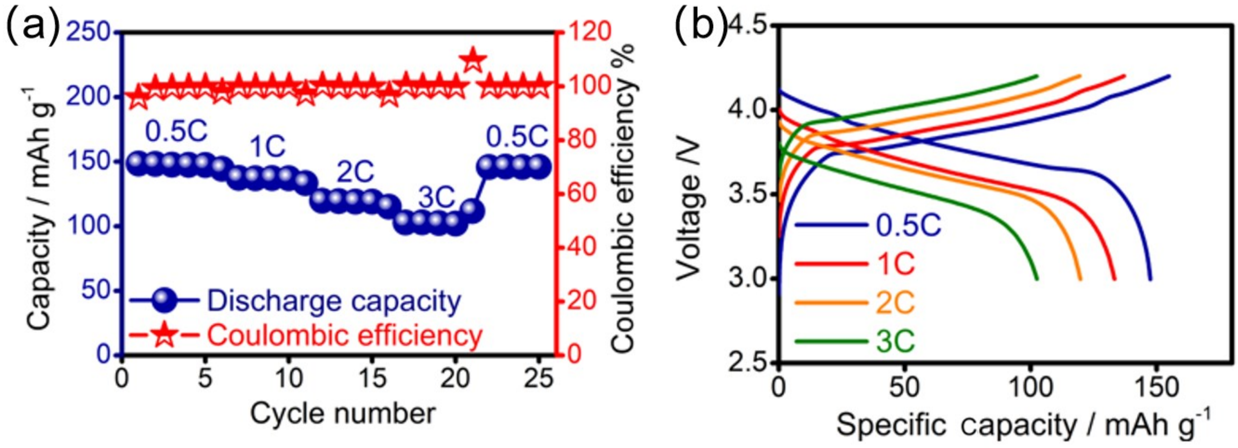

Figure S7. (a) Rate performance and (b) corresponding galvanostatic charge-discharge profiles of flexible cell with cubic units.

Supplementary note 2

3. Calculations of energy density

3.1 Calculations of energy density of the battery with cubic units

Volume = 101.88 mm × 21.95 mm × 2.63 mm = 5.88 cm^3

The capacity and average voltage of the battery with cubic units are 577 mAh and 3.79 V, respectively.

Specific capacity = 260/3.12 cm^3 = 98.12 mAh/cm^3

Energy density = 3.79 V × 98.12 mAh/cm^3 = 371.9 Wh/L.

3.2 Calculations of energy density of the conventional pouch cell

Volume = 100.86 mm × 18.35 mm × 3.03 mm = 5.6 cm^3

The capacity and average voltage of the battery with cubic units are 601 mAh and 3.73 V, respectively.

Specific capacity = 601/5.6 cm^3 = 107.3 mAh/cm^3

Energy density = 3.73 V × 107.3 mAh/cm^3 = 400.3 Wh/L.

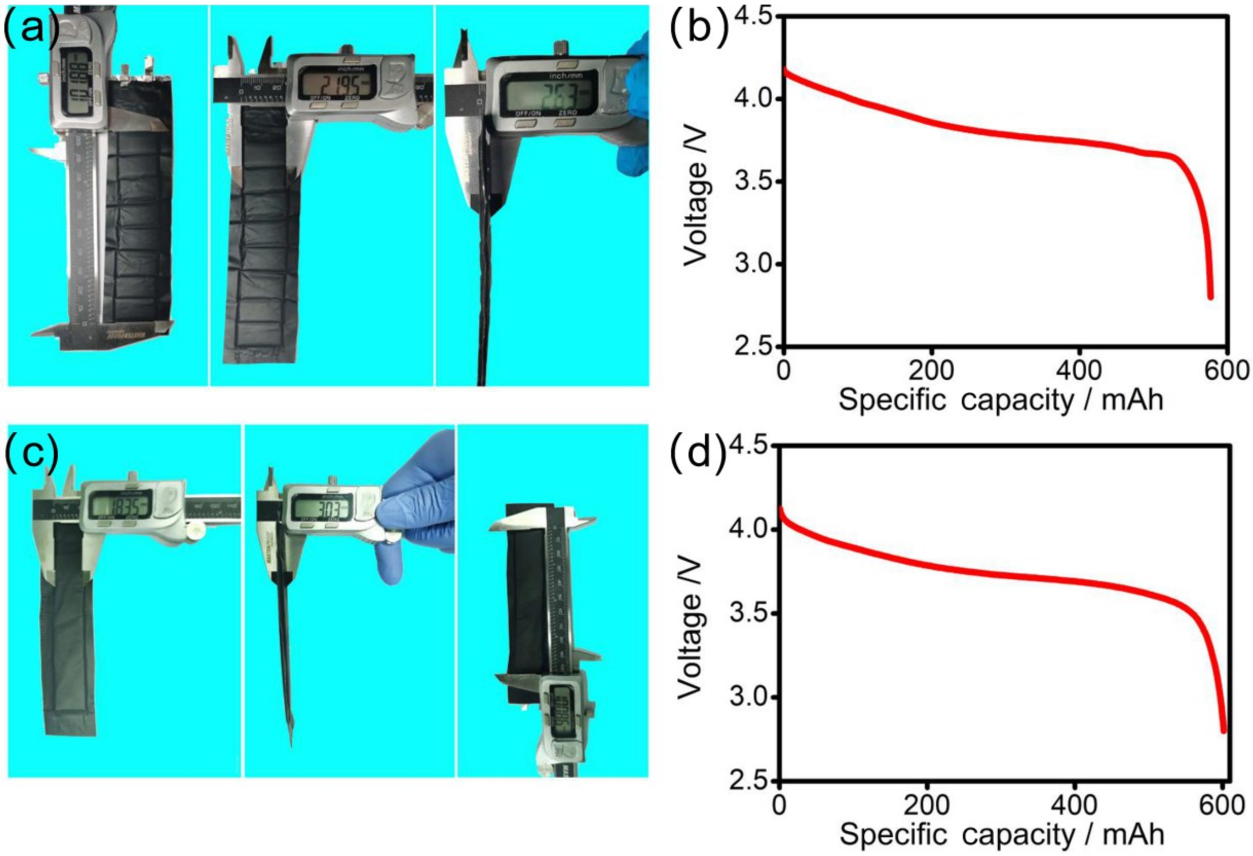

Figure S8. (a) Size of battery with cubic units. (b) Discharge capacity of battery with cubic units. (c) Size of conventional pouch cell. (d) Discharge capacity of conventional pouch cell.

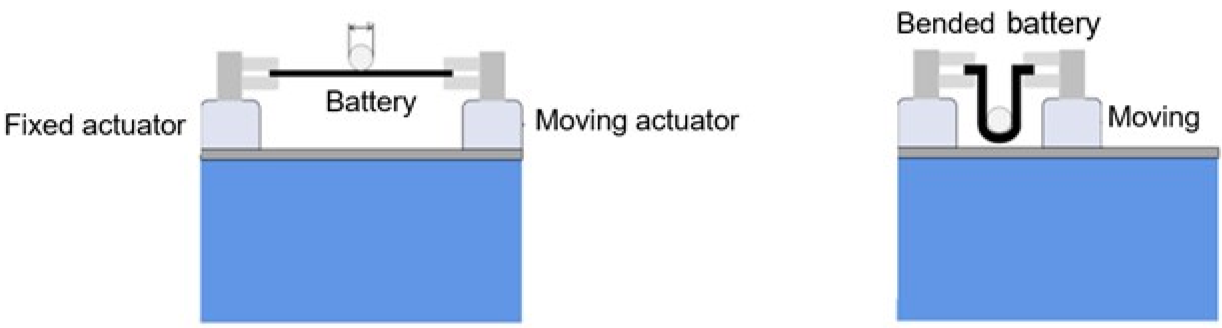

Figure S9. The schematic of the custom-made bending apparatus. The Teflon cylinder is used to control bending radius.

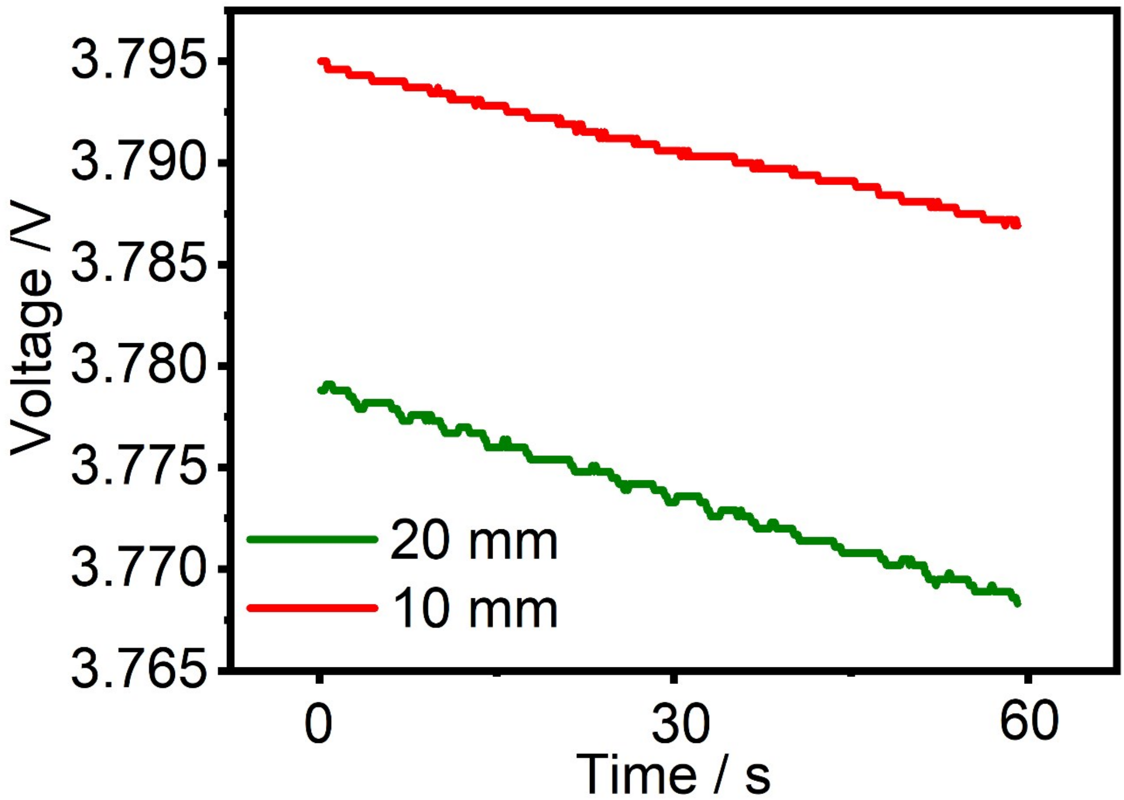

Figure S10. Amplified voltage profiles of the cell under dynamic bending with 20 mm and 10 mm bending radius.

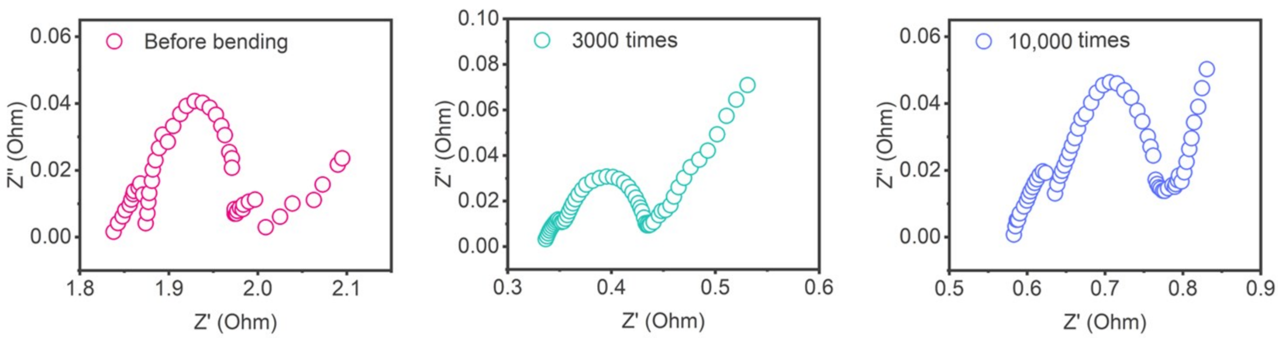

Figure S11. The Nyquist plots of the (electrochemical impedance spectroscopy) EIS measurements taken before and after 3,000 and 10,000 bending of battery with cubic units.

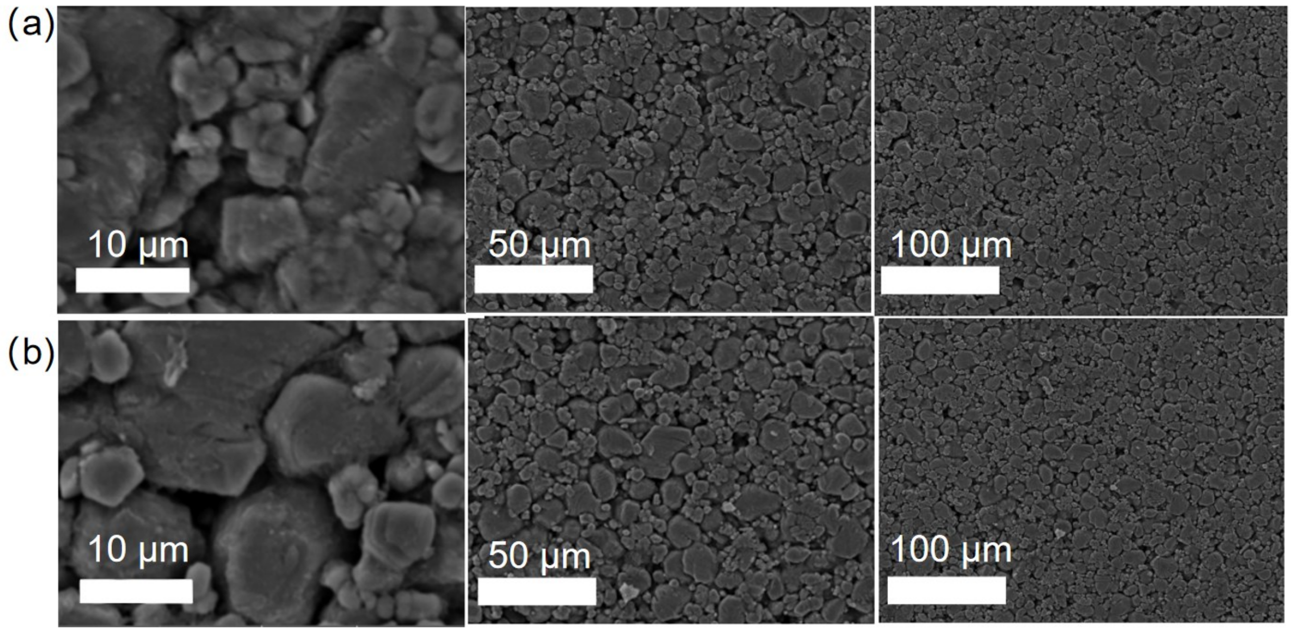

Figure S12. Scanning electron microscopy (SEM) images of the electrodes (a) before and (b) after dynamic bending test.

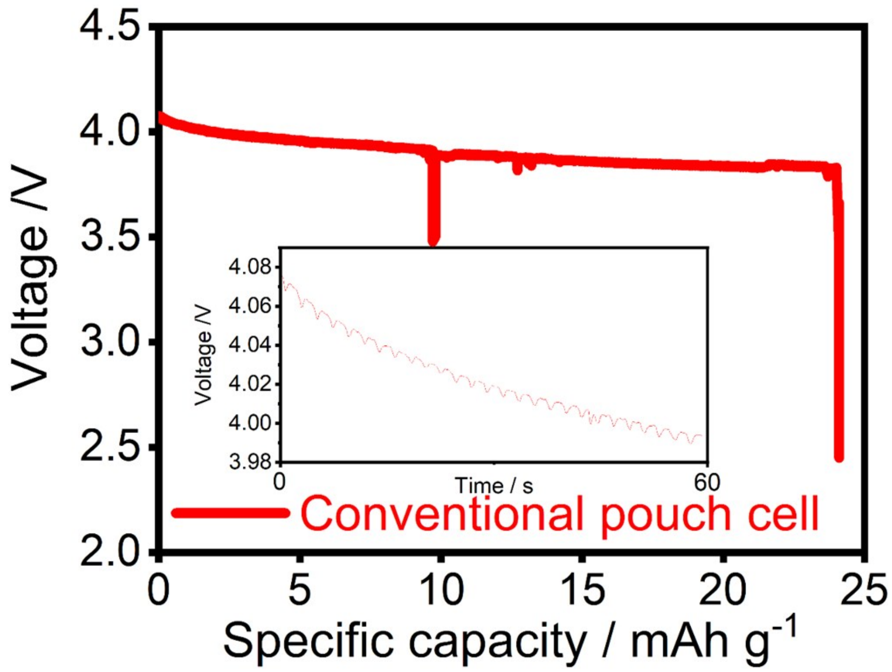

Figure S13. The galvanostatic discharge voltage profile of conventional pouch cell under dynamic bending and amplified discharge profile.

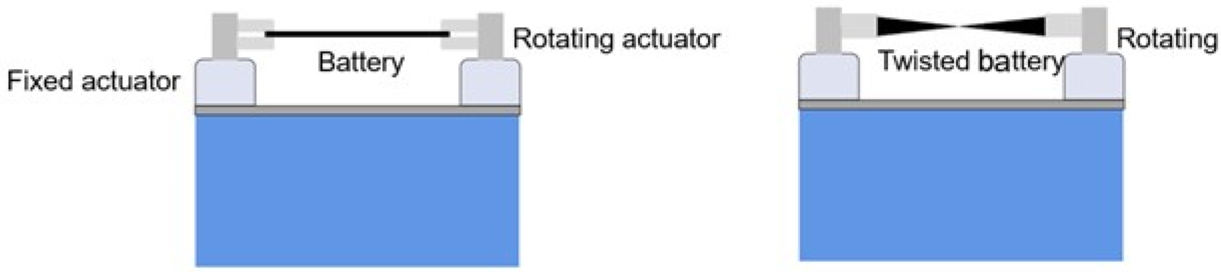

Figure S14. The schematic of the custom-made torsion apparatus.

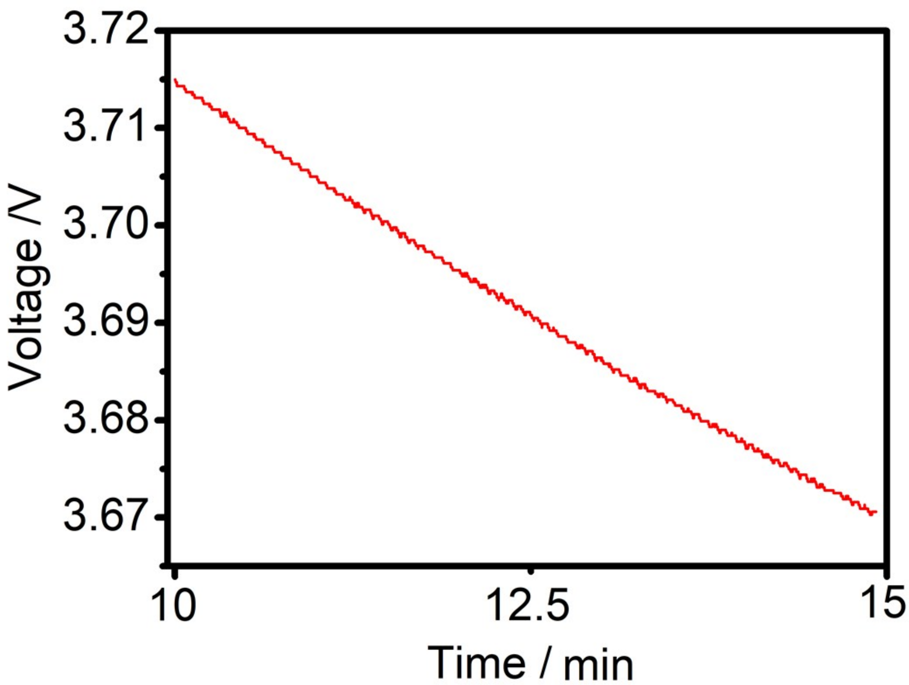

Figure S15. The amplified voltage profile of the cell under dynamic torsion.

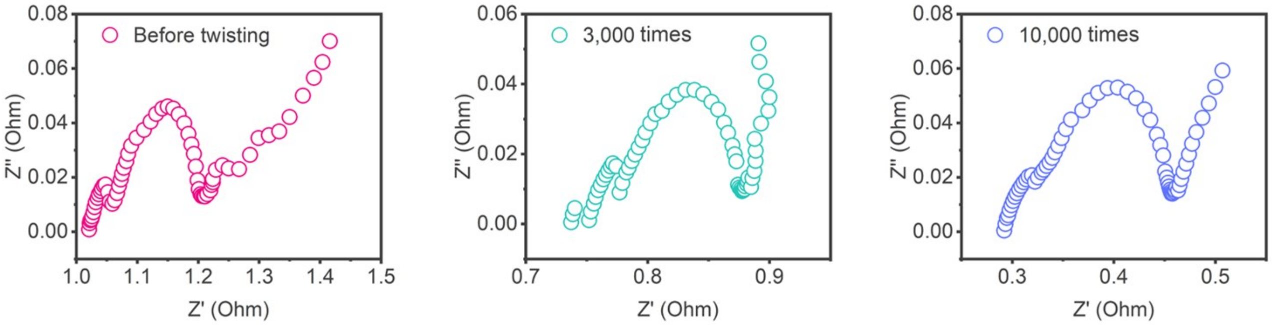

Figure S16. The Nyquist plots of the (electrochemical impedance spectroscopy) EIS measurements taken before and after 3,000 and 10,000 twisting of battery with cubic units.

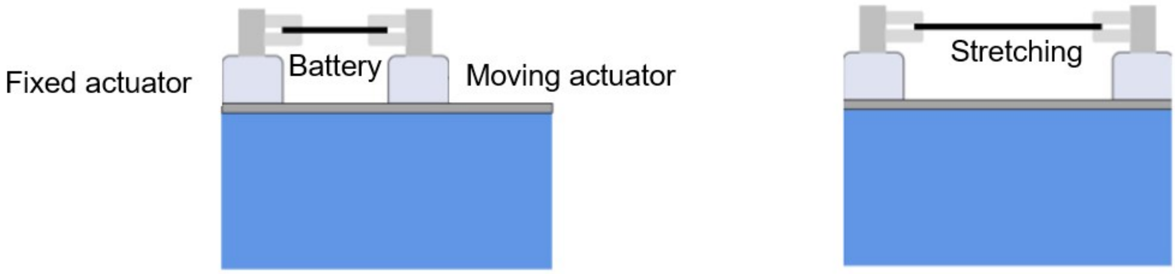

Figure S17. The schematic of the custom-made stretching apparatus.

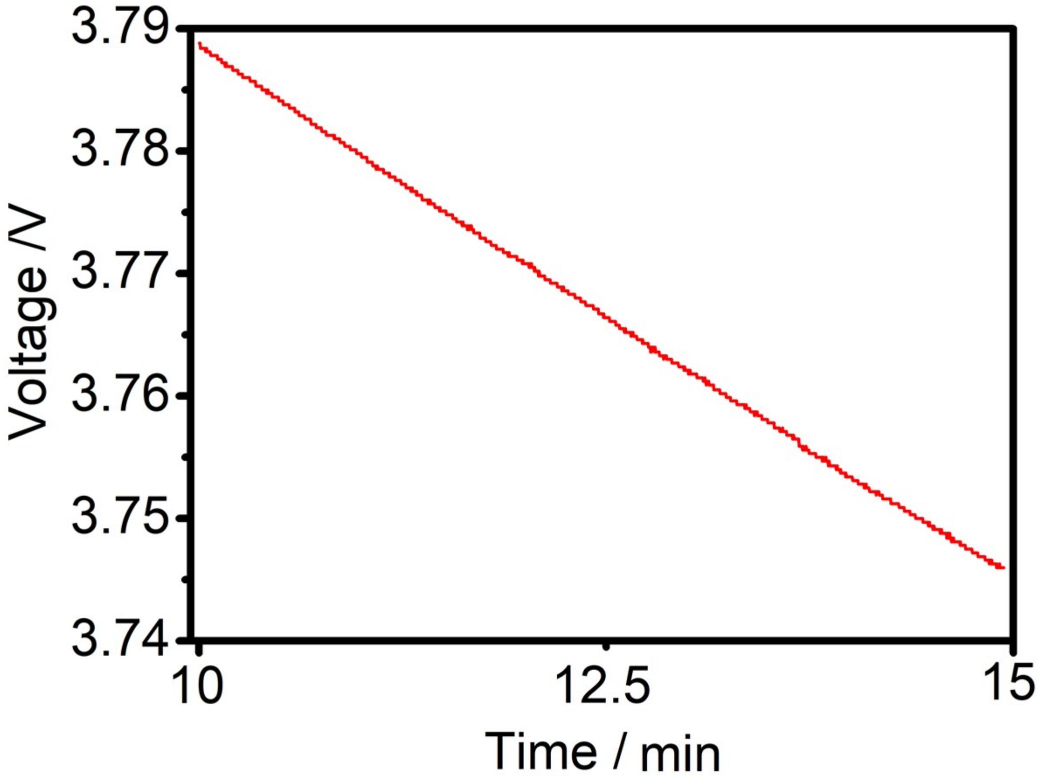

Figure S18. The amplified voltage profile of the battery with cylindrical units under dynamic stretching.

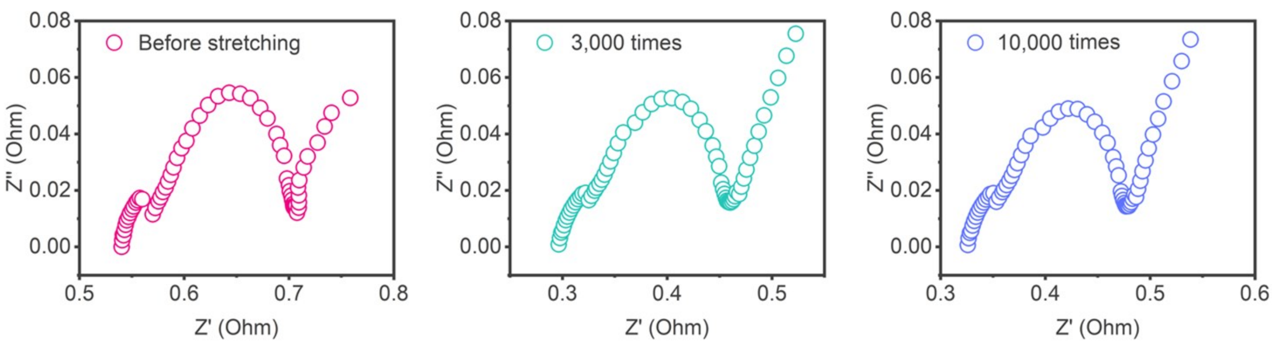

Figure S19. The Nyquist plots of the (electrochemical impedance spectroscopy) EIS measurements taken before and after 3,000 and 10,000 stretching of battery with cylindrical units.

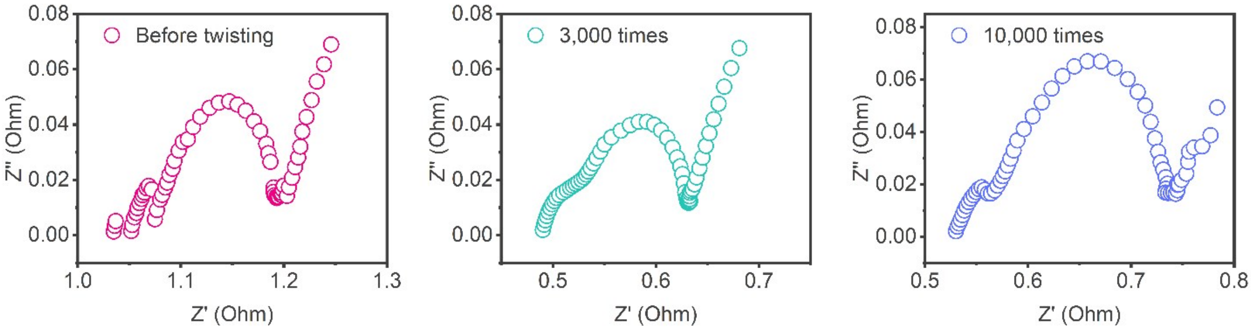

Figure S20. The Nyquist plots of the (electrochemical impedance spectroscopy) EIS measurements taken before and after 3,000 and 10,000 twisting of battery with cylindrical units.

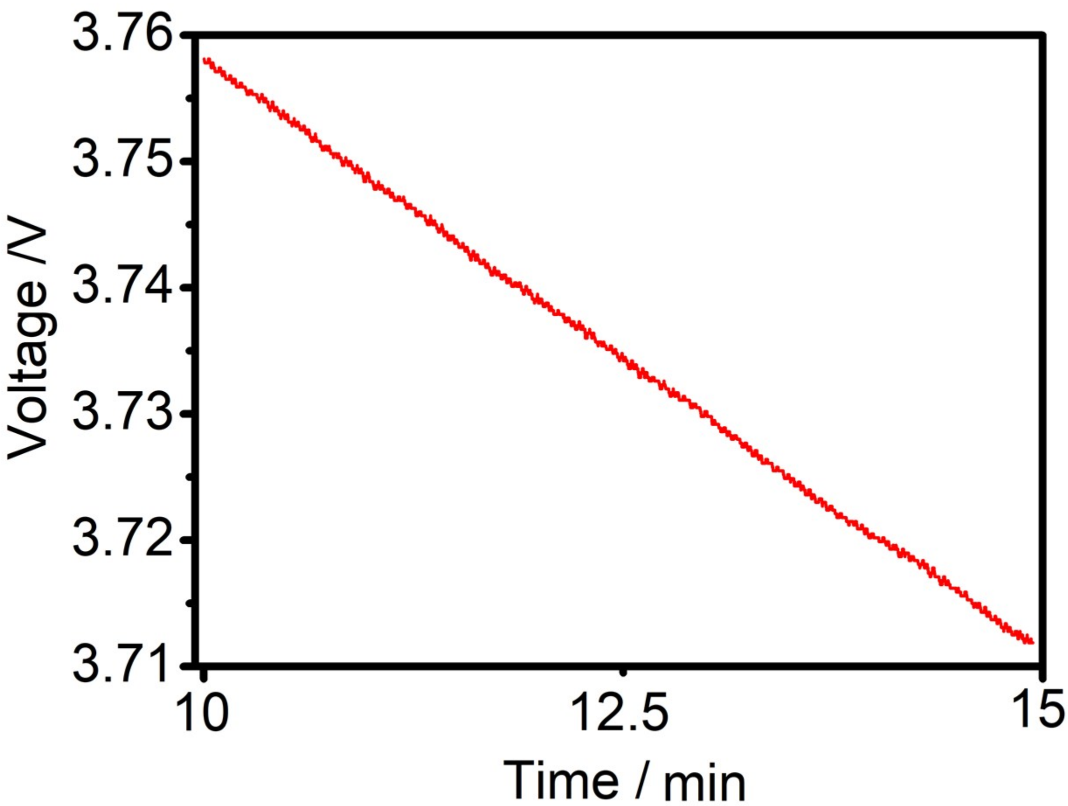

Figure S21. The amplified voltage profile of the battery with cylindrical units under dynamic twisting.

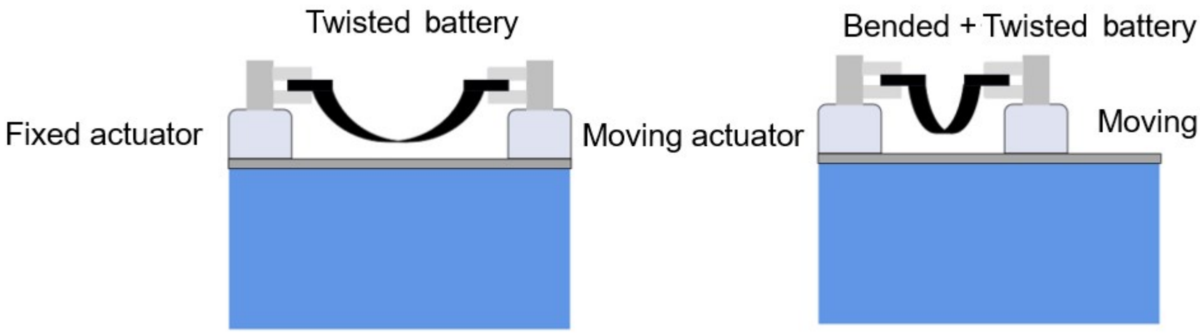

Figure S22. The schematic of the custom-made bending+torsion apparatus.

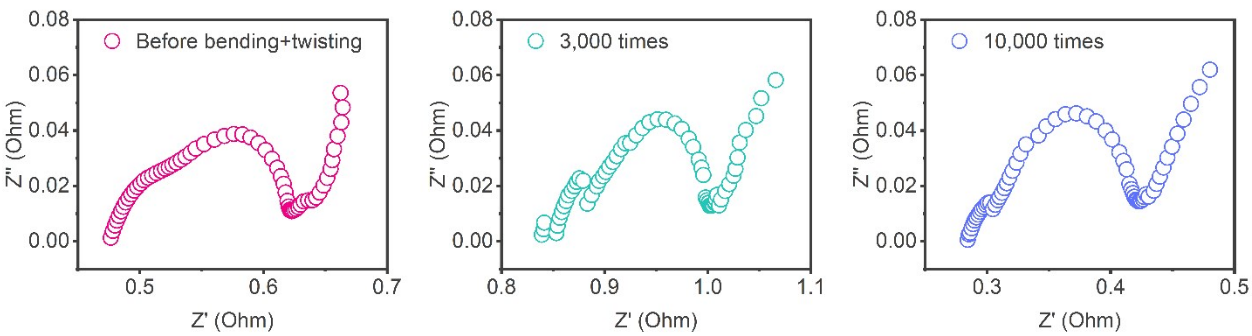

Figure S23. The Nyquist plots of the (electrochemical impedance spectroscopy) EIS measurements taken before and after 3,000 and 10,000 bending+twisting of battery with cylindrical units.

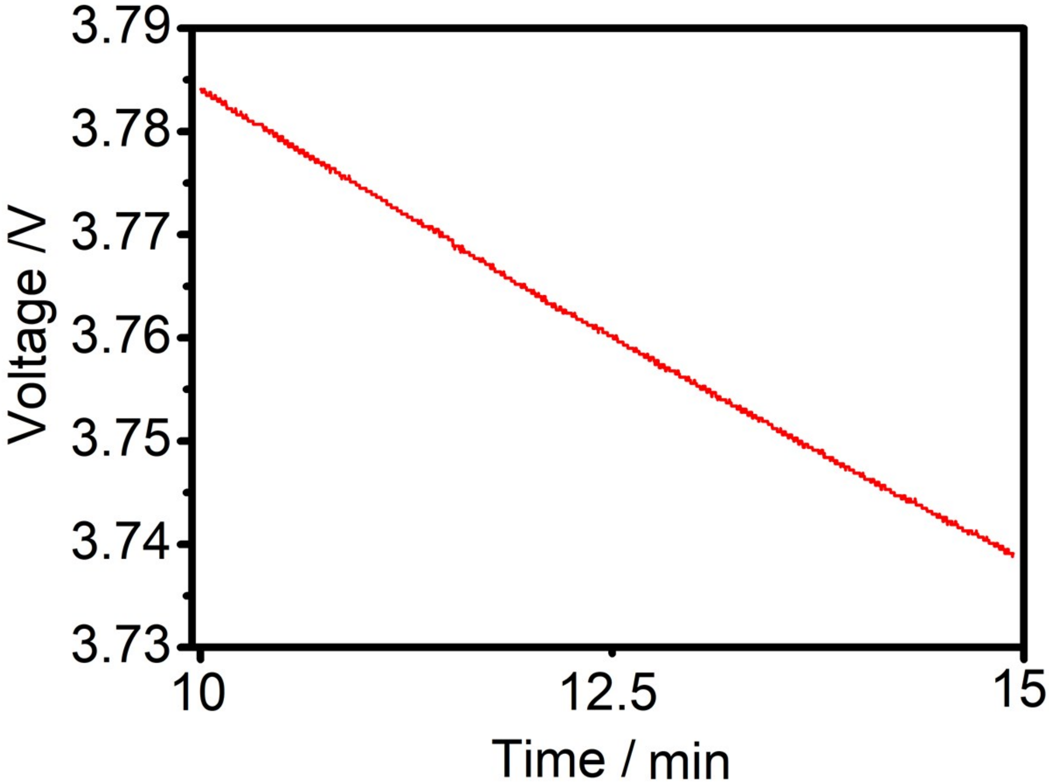

Figure S24. The amplified voltage profile of the battery with cylindrical units under dynamic bending+twisting.

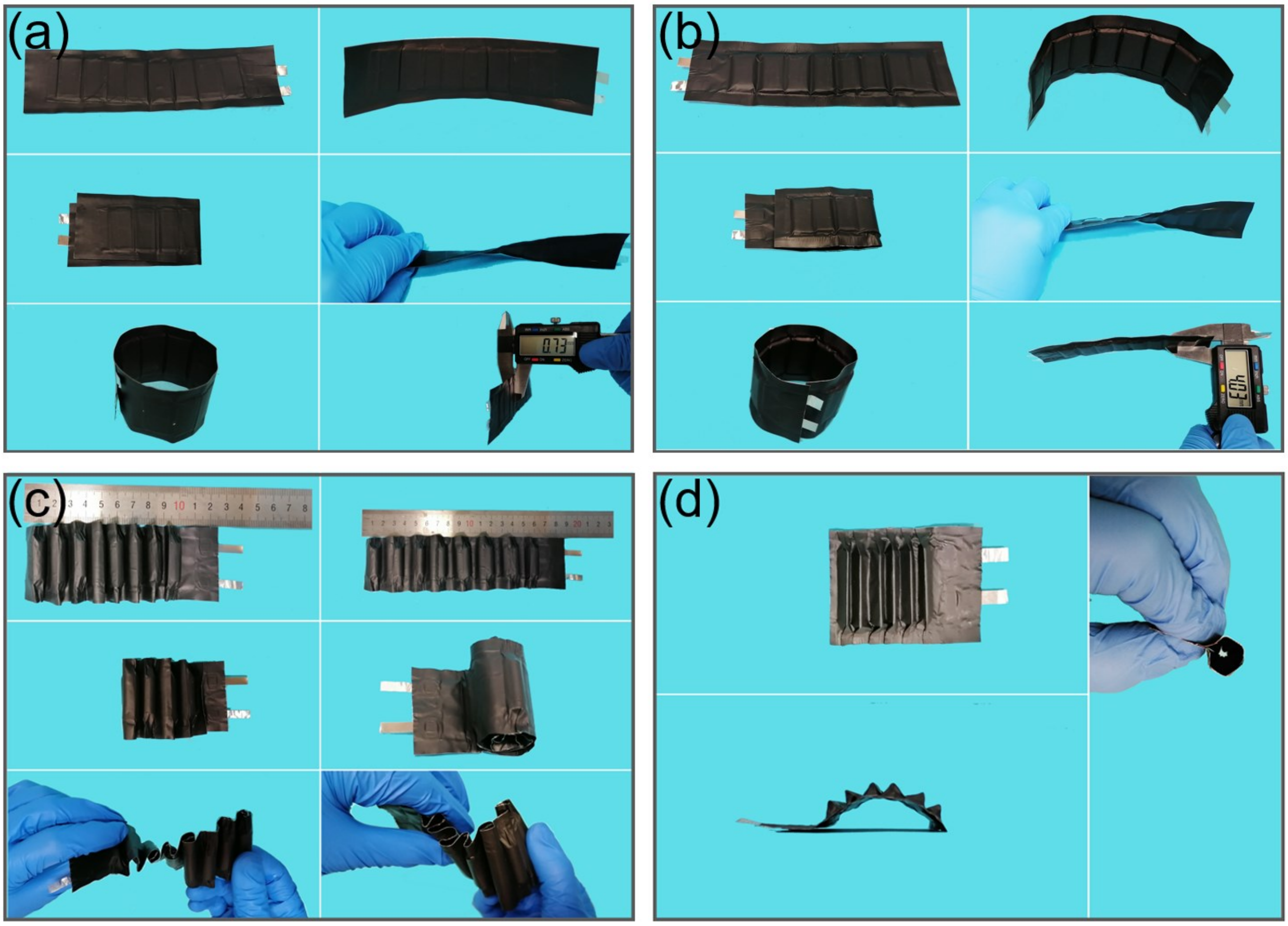

Figure S25. Various deformations for (a) the battery with a thickness of 0.73 mm cubic units and (b) the battery with a thickness of 4.03 mm cubic units. (c) The battery with bigger cylindrical units can also achieve stretching, folding, winding, twisting and bending+twisting deformations. (d) The bending and winding deformations for battery with smaller size of triangular prism shaped units.

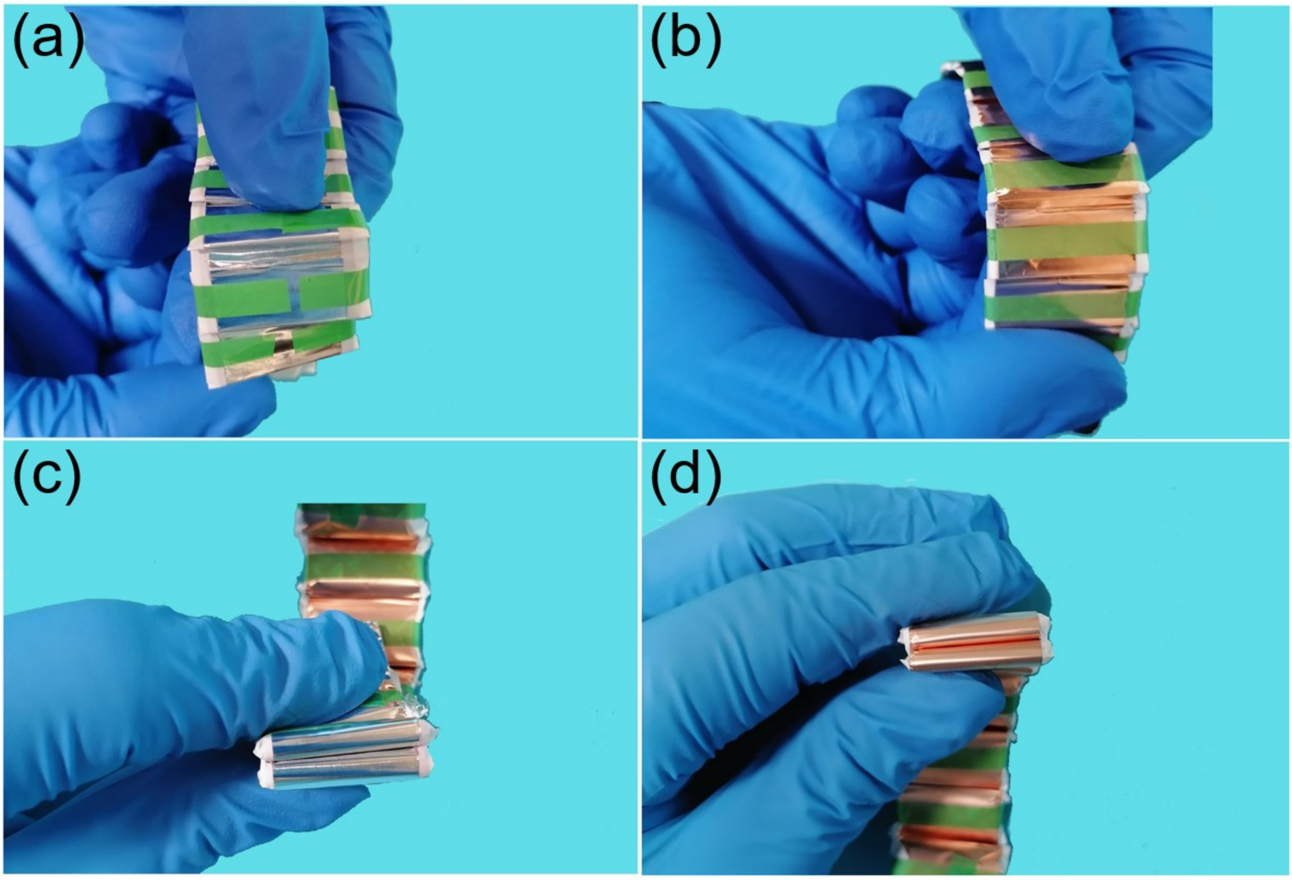

Figure S26. (a,b) The optical images of Al and Cu foils after 1,000 times bending of the battery with thin units. (c,d) The optical images of Al and Cu foils after 1,000 times bending of the battery with thick units.

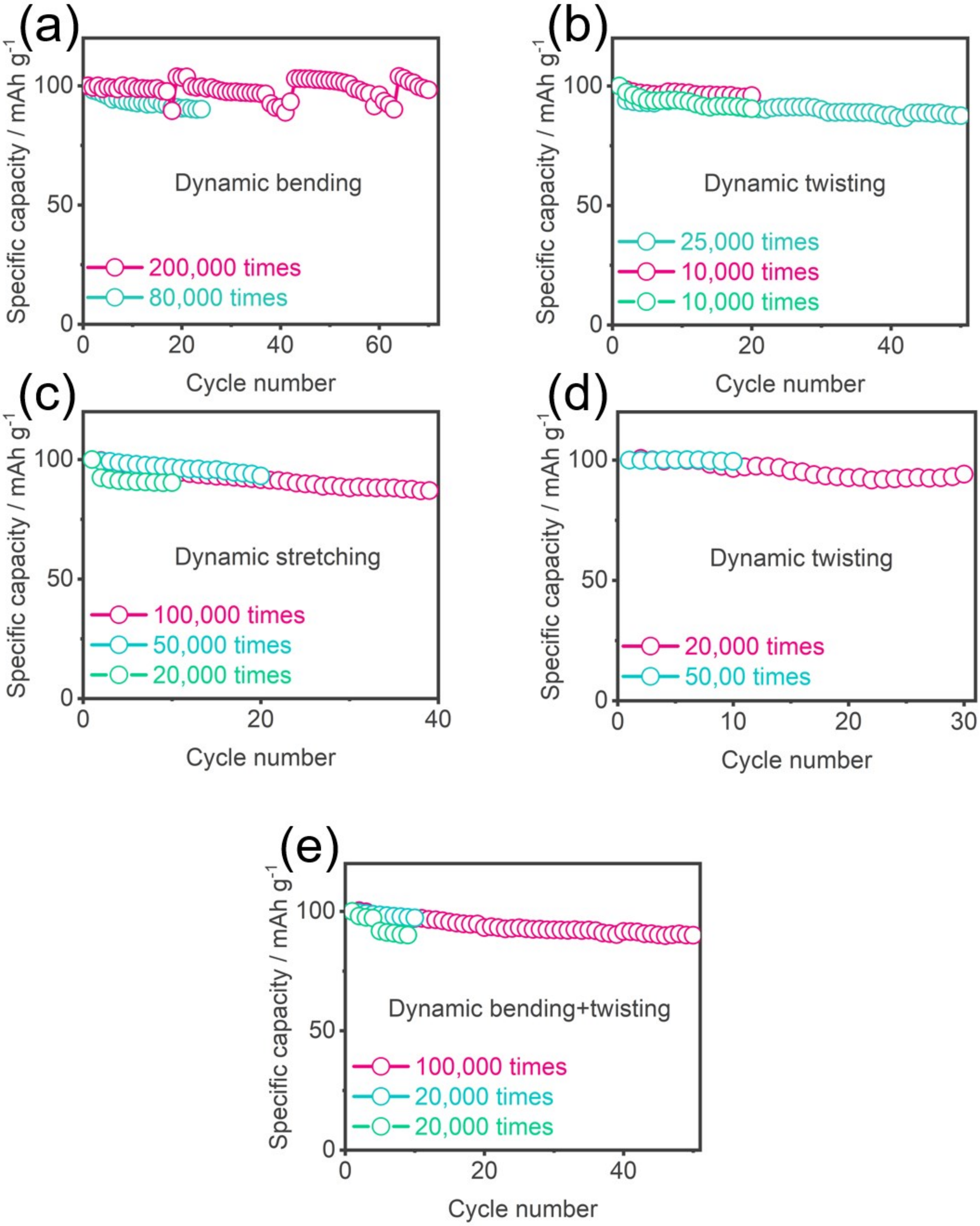

Figure S27. Capacity retentions of batteries with cubic units under (a) dynamic bending and (b) dynamic twisting. Capacity retentions of batteries with cubic units under (a) dynamic stretching, (b) dynamic twisting and (c) bending+twisting.